

<https://doi.org/10.2298/SOS220723019G>

*Submitted: 23.07.2022.*

*Accepted for publication: 15.09.2022.*

**UDK: 546.831; 692.533.1**

**PROCESSING OF GELATINE COATED COMPOSITE  
SCAFFOLDS BASED ON MAGNESIUM AND STRONTIUM  
DOPED HYDROXYAPATITE AND YTTRIA-STABILIZED  
ZIRCONIUM OXIDE**

Aleksa Galić<sup>1</sup>, Tamara Matić<sup>2</sup>, Nataša Obradović<sup>2</sup>,  
Zvezdana Baščarević<sup>3</sup>, Djordje Veljović<sup>1\*</sup>

<sup>1</sup>*University of Belgrade, Faculty of Technology and Metallurgy, Karnegijeva 4, 11000  
Belgrade, Serbia*

<sup>2</sup>*Innovation Center of Faculty of Technology and Metallurgy, Karnegijeva 4, 11000  
Belgrade, Serbia*

<sup>3</sup>*University of Belgrade, Institute for Multidisciplinary Research, Kneza Višeslava 1,  
11000 Belgrade, Serbia*

\*Corresponding author: Djordje Veljović: [djveljovic@tmf.bg.ac.rs](mailto:djveljovic@tmf.bg.ac.rs)

**Abstract**

Limited bone bank capacity and risk of infection are some of the main drawbacks of autologous and allogenic grafts, giving rise to synthetic materials for bone tissue implants. The aim of this study was to process and evaluate the mechanical properties and bioactivity of magnesium and strontium doped hydroxyapatite (HAp) scaffolds and investigate the effect of adding zirconium oxide and gelatine coating the scaffolds. Doped nanosized hydroxyapatite powder was synthesized by the hydrothermal method and the scaffolds were made by the foam replica technique and sintered at different temperatures. Yttria-stabilized zirconium oxide (YSZ), synthesized by plasma technology, was used as reinforcement of calcium phosphate scaffolds. Element analysis, phase composition, morphology of the powders and microstructure of

the scaffolds were investigated, as well as the compressive strength of the coated and uncoated scaffolds and bioactivity in simulated body fluid (SBF). A microporous structure was achieved with interconnected pores and bioactivity in SBF was confirmed in all cases. The best mechanical properties were given by the coated composite HAp/YSZ scaffolds, withstanding average stresses of over 1019 kPa. These results encourage the idea of use of these scaffolds in bone regenerative therapy and bone tissue engineering.

**Keywords:** hydroxyapatite, scaffolds, zirconium oxide, composite, tissue engineering.

## 1. Introduction

With an increased number of bone defects needed to be treated, due to an aging world population, decrease in physical activity and more prevalent cases of obesity, resulting in skeletal disorders, surgical bone transplantation presents a solution for numerous defects such as osteonecrosis, tumors, big fractures and can be used in spinal fusion surgery [1-2]. Autologous and allogenic bone grafts, while still being the gold standard for these operations [3], do possess some major drawbacks. As autologous grafts are taken from the patient, usually from the iliac crest, this can result in additional pain for the patient and further complications in the procedure [4]. Aside from this, there is a limited number of grafting sites which are suitable. The use of allogenic grafts, where bone tissue is harvested from a donor, is hindered by limited bone bank capacities and risk of immunological reaction and infection [5]. These problems give rise to synthetic materials with engineered properties for specific use as bone implants, with an increasing number of researchers devoting their research to this topic [6]. Among others, one of the predominant materials used for these purposes is calcium hydroxyapatite. Hydroxyapatite is the main mineral constituent of bone tissue, which attributes to its biocompatibility, bioactivity, and non-toxic properties [2,7]. Research has also show that it is inert and able to bond with biological bone [8]. Within the hydroxyapatite structure are present easily interchangeable calcium ions, which are partially substituted with magnesium and strontium ions in this study. Magnesium was chosen as a dopant because of its stabilizing effect on the  $\beta$ -tricalcium-phosphate phase ( $\beta$ -TCP) during sintering, as it is shown to increase the temperature needed for the transition into  $\alpha$ -tricalcium-phosphate ( $\alpha$ -TCP) [9,10]. It has also been found that it

promotes the interaction between osteoblasts and the implanted material, elevates bone mineralization, heightens antimicrobial activity and increases the hardness and toughness of the ceramic material [11]. Magnesium has been reported to increase cell differentiation and proliferation [12]. Strontium ions were used as they are shown to promote solubility of the hydroxyapatite, which is essential for bone tissue engineering purposes and the bioactivity of the material. Strontium ions are also shown to increase the antibacterial effects of the hydroxyapatite and decrease the size of the hydroxyapatite particles [2,13]. Hydroxyapatite co-doping with strontium alongside magnesium ions was found to favor the formation of the  $\beta$ -TCP phase and stabilize it, while suppressing the transformation into  $\alpha$ -TCP [14]. Other research suggests the stress induced by the magnesium ions in the crystal lattice can be compensated for with the incorporation of strontium ions, thus stabilizing the structure [15]. It has also been shown that that co-doping with magnesium and strontium leads to greater cell differentiation [16]. Since biological hydroxyapatite is not stoichiometric [17], a Ca/P of less than 1.67 was used in this research as well, replacing phosphate groups with carbonate groups. In order to integrate with the surrounding tissue, the implanted biomaterial must mimic the bone morphology. To address this, a porous structure is crucial to be achieved, as it is needed to promote osteoconduction and proliferation of the cells, with studies showing that a minimum pore size of 100  $\mu\text{m}$  is needed for tissue engineering applications [18]. On the other hand, with increased porosity, the mechanical properties of the scaffolds are declined. In order to compensate for this, yttrium-stabilized zirconia (YSZ), as a biocompatible and bio-inert material with great fracture toughness properties, was used to achieve a greater compressive strength of the obtained scaffolds [19]. In addition to this, the mechanical properties can further be enhanced by coating the scaffolds with a biocompatible polymer, such as gelatine. Being a form of denatured collagen, the role of gelatine is to temporarily fill in the cracks and cavities in the ceramic structure of the hydroxyapatite-based scaffolds, thus bettering its mechanical properties, before being resorbed [20].

The aim of this study was to process and evaluate the mechanical properties and bioactivity of scaffolds based on magnesium and strontium doped hydroxyapatite, as well as investigate the effect of adding yttria-stabilized zirconium oxide and gelatine

coating the scaffolds for application in bone regenerative therapy and bone tissue engineering.

## **2. Experimental procedures**

### **2.1. Synthesis of doped hydroxyapatite**

Hydroxyapatite powder, doped with 4 mol.% of magnesium and 1 mol.% of strontium (Mg<sub>4</sub>Sr<sub>1</sub>-HAp), was synthesized using the modified hydrothermal method, described earlier [14, 21]. The precursors used were: calcium-nitrate tetrahydrate (Acros Organics B.V.B.A., India, > 90 %), disodium ethylenediaminetetraacetate (Acros Organics B.V.B.A., Spain, > 99 %), sodium-dihydrogen phosphate (VWR Chemicals BDH, Belgium, 99,8 %), urea (Acros Organics B.V.B.A., Germany, 99,5 %), magnesium-nitrate hexahydrate (CARLO ERBA Reagents GmbH, France, 98,0 %), strontium-nitrate (Keramika, Yugoslavia, > 99 %). The initial Ca/P ratio was 1.52. The precursors for the synthesis and their amounts are shown in Table I:

#### **Tab.I**

The reactants were dissolved in 1.5 dm<sup>3</sup> of deionized water in the order given above in an Erlenmeyer flask with constant mixing and then transferred in an autoclave filled with 1.5 dm<sup>3</sup> of deionized water. The solution was subject to a temperature of 160°C and pressure of 8 bar inside the autoclave for 3h, after which it was left to cool for 24h to room temperature. Excess water was decanted and the Mg<sub>4</sub>Sr<sub>1</sub>-HAp powder was filtered using a Büchner funnel. The powder was dried for 2 h at 105°C. The doped hydroxyapatite powder was calcined at 1000°C for 4 h with the heating rate of 20°C/min. Yttria-stabilized zirconium oxide (YSZ) was previously synthesized using plasma technology [22].

### **2.2. Scaffolds fabrication**

The ceramic scaffolds were made using the foam replica method [20, 23-25]. The paste used to infiltrate the polymer foam was made by mixing the Mg<sub>4</sub>Sr<sub>1</sub>-HAp powder with polyvinyl alcohol (PVA, Sigma-Aldrich, Germany) solution which was used as the dispersing agent [24, 26-27]. The paste consisted of 30 wt.% Mg<sub>4</sub>Sr<sub>1</sub>-HAp, 3 wt.%

PVA and 67 wt.% deionized water. For the composite samples, zirconium oxide was also added by substituting 20wt% of the Mg4Sr1-HAp in the paste with YSZ. Mixing was done on a magnetic stirrer at 80°C [24, 25]. The paste was then treated with ultrasound for 2 min in order to get a homogeneous suspension.

Since the zirconia powder consisted of different size particle fractions [28] sedimentation was used in order to extract only the finer particle fractions. YSZ was suspended in deionized water and treated with ultrasound for 10 min and left still for 1 min. After sedimentation, 0.2 ml of the suspension was pipetted out and dried in order to determine the weight fraction of YSZ after sedimentation.

The polyurethane foam was dipped into the paste and mixed so that the paste would infiltrate inside the pores of the foam. All the excess paste was removed and the samples were left to dry for 48 h at room temperature. The pre-sintered scaffolds are shown in Fig. 1.

### **Fig.1.**

Two step sintering was used for all the samples. The scaffolds were slowly heated for 6 h at a heating rate of 2 °C/min to the temperature of 750°C which was kept constant for 20 min in order to decompose the foam without damaging the scaffold structure, similar to the study done by Liu et al. [29] and Dressler et al. [30], after which the scaffolds were again heated for 1h to the higher sintering temperatures of 1400, 1430 and 1470°C where they were held for 2 h. After sintering the scaffolds noticeably shrank, as seen in Fig. 2. From both sample groups 6 scaffolds were made at each sintering temperature.

### **Fig. 2.**

### **2.3. Gelatine coating**

When coating the scaffolds with gelatine, a 5 wt.% solution of bovine gelatin (Type B bovine skin gelatine, Sigma-Aldrich, Germany) was prepared. The scaffolds were dipped in the gelatine at 60°C and left to soak for 1h, after which all the excess gelatine was removed. The Mg4Sr1-HAp scaffolds sintered at 1430 °C exhibited

satisfactory mechanical properties, hence they were chosen to be coated with gelatine. The Mg<sub>4</sub>Sr<sub>1</sub>-HAp/YSZ scaffolds showed best compressive strength after sintering at 1470 °C, but it was decided to sinter them at 1500°C before gelatine coating, with the hypothesis that this would lead to even better densification and, as a consequence, the improvement of the mechanical properties.

#### **2.4. Characterisation**

Elemental analysis was done using energy dispersive spectroscopy (EDS) on an INCAPentaFETx-3 coupled with a Tescan Vega TS 5130MM scanning electron microscope, operated at 20 keV. These values were acquired as the mean of 4 separate measurements. Phase composition of the calcined powder and the scaffolds was determined by X-ray diffraction analysis (XRD) on a Rigaku Smartlab diffractometer in the 2 $\theta$  angle ranging from 20° to 50°, with a scan rate of 0.02° s<sup>-1</sup>. Phase identification was done by comparing the experimental XRD patterns with standards compiled by the Joint Committee on Powder Diffraction Standards cards, JCPDS 09–0432, JCPDS 09–0169, JCPDS 09–0348 and JCPDS 80-0965 for HAP,  $\beta$ -TCP,  $\alpha$ -TCP and tetragonal zirconia phases respectively. Quantitative analysis of the phase compositions was performed using the PowderCell software. The morphology of the powder and microstructure of the scaffolds was observed using a TESCAN MIRA 3 XMU scanning electron microscope, operated at 20 keV. All samples were previously coated with a thin layer of gold. The compressive strength of all scaffolds was tested on a Shimadzu, Universal Testing Machine, AG-X Plus at a strain rate of 5 mm/min until 10% deformation. The bioactivity of the uncoated samples was evaluated after soaking in simulated body fluid (SBF) for 7 days at 37 °C, while renewing the fluid every 2 days.

### **3. Results and discussion**

SEM analysis showed the powder being composed of nanoscale needle-like shaped particles, grouped into clusters which formed hollow spherical agglomerates around 1  $\mu$ m in size (Fig. 3a). The morphology of calcined powder showed densification occurring inside the particles themselves as well as the occasional merging of the particles (Fig. 3b).

**Fig.3.**

The results of elemental analysis of the Mg<sub>4</sub>Sr<sub>1</sub>-Hap powder showed a Ca/P ratio of 1.31, while the fraction of the doping Mg and Sr atoms were 0.40 and 0.66 at.%, respectively indicating higher substitution affinity of Sr ions, which is in good agreement with the previously reported results [14].

The diffractogram of the calcined Mg<sub>4</sub>Sr<sub>1</sub>-Hap powder (Fig. 4) showed a biphasic system with the predominant  $\beta$ -TCP phase, containing 37 % HAp and 63 %  $\beta$ -TCP (Table II). High  $\beta$ -TCP phase content of calcinated Mg<sub>4</sub>Sr<sub>1</sub>-Hap powder was expected due to the phase transformation of HAp in to the  $\beta$ -TCP when thermally treated above 800 °C. Additionally, the presence of Mg ions in the HAP structure is known to further promote the HAp- $\beta$ -TCP phase transition.

**Fig.4.****Tab.II**

After sintering at 1400 °C, a triphasic scaffold material was obtained with the hydroxyapatite as the major phase, presumably due to the partial transformation of the existing  $\beta$ -TCP into  $\alpha$ -TCP phase upon heating above 1125 °C (shown in the Fig. 5a). As expected, a further increase of the sintering temperature to 1430 °C resulted in increased transformation of HAp into  $\beta$ -TCP phase, as shown in the Fig. 5b and Table II.

**Fig.5.**

Even further decomposition of the hydroxyapatite phase is observed when sintering at 1470 °C (Fig. 6). Very low intensity peaks of hydroxyapatite are present in the composite Mg<sub>4</sub>Sr<sub>1</sub>-HAp/YSZ scaffold, with  $\beta$ -TCP and  $\alpha$ -TCP being the predominant phases in the calcium phosphate (CaP) matrix. The high intensity peaks, attributed to tetragonal phase of zirconium oxide showed the successful inclusion of zirconia inside the CaP matrix hydroxyapatite matrix.

**Fig.6.**

Both sample groups of the uncoated scaffolds had interconnected pores with the average size of 250  $\mu\text{m}$  (Fig. 7), which would support vascularization, proliferation and osteoconduction of the cells that would be here in practice, as stated by Sopyan et al. [23]. Inside the columns of the scaffolds, visible voids can be seen (Fig. 6b) as a result of the polymer foam occupying these voids prior to sintering, which is in line with the findings of Dressler et al. [30]. This is one of the weak spots of the foam replica process but can be overcome by coating the scaffolds with a polymer [31].

**Fig.7.**

The mechanical properties of the uncoated scaffolds are shown in Fig. 8. As can be seen, the Mg4Sr1-HAp scaffolds exhibited highest values of compressive strength after sintering at 1400 °C and 1430°C, the prior group with standing stresses up to 87 kPa.

**Fig.8.**

A significant drop in strength can be seen after sintering at 1470°C. This can be attributed to the phase transition of existing  $\beta$ -TCP at higher temperatures into the  $\alpha$ -TCP phase, which is known to be a mechanically weaker phase [32]. Moreover, the crack formation in the structure as a result of the higher volume of the formed  $\alpha$ -TCP phase also attributed to the decrease in compressive strength, which is in line with the findings of Bohner et al. [33]. The composite scaffolds sintered at the lower temperatures showed very poor compressive strength, due to inadequate densification occurring at these temperatures. With the increase in temperature, densification rate also increased, and when sintering at 1470°C, the composite scaffolds with stood stresses up to 65 kPa. Despite the increase in compressive strength, these values were still lower than those for the Mg4Sr1-HAp scaffolds, suggesting the need for even higher sintering temperatures. Significantly lower values of compressive strength can be explained by the lower densification compared to the Mg4Sr1-HAp scaffolds, as it is shown in the



Fig. 9. A possible explanation for this, according to prior studies, is that the addition of zirconium oxide hinders the movement of grain boundaries, raising the temperature needed for sintering [34].

**Fig.9.**

An increase in compressive strength can be achieved by coating the scaffolds with a biocompatible polymer, which would fill in the gaps and fractures in the scaffolds structure, as shown by Kim et al. [20] and Philippart et al. [31].

After coating the scaffolds with gelatine, a significant increase in compressive strength was observed. The doped Mg4Sr1-HAp scaffolds sintered at 1430°C more than doubled in strength, reaching 207 kPa in comparison to the 87 kPa achieved with the uncoated scaffolds. The composite scaffolds, after being sintered at a slightly higher temperature of 1500 °C and coated with gelatine exhibited an increase in strength by over 15 times. The gelatine coated composite scaffolds had a mean compressive strength of 1019 kPa with maximal stress reaching 1843 kPa. This major increase in strength can be explained through the means of higher densification occurring at this sintering temperature, which is supported by the fact that visibly higher shrinkage occurred after sintering of these scaffolds. Aside from this, the gelatine coating probably had the major role in strength increase, by infiltrating all the cracks and voids in the scaffold microstructure.

After 7 days of incubation in Kokubo simulated body fluid, [35] the doped Mg4Sr1-HAp scaffolds, which were sintered at 1400°C showed greater coverage with the newly former needle-like hydroxyapatite phase in comparison with the composite scaffolds, sintered at 1470 °C, which were only partially covered (Fig. 10). These results indicate to the higher bioactivity of the doped Mg4Sr1-HAp scaffolds but suggest that both sample groups could potentially be used *in vivo* in bone tissue engineering applications.

**Fig.10.**

#### 4. Conclusion

Elemental analysis of synthesized HAp powders showed a mean Ca/P ratio of 1.31 and the presence of Mg and Sr atoms. Macroporous scaffolds based on Mg<sub>4</sub>Sr<sub>1</sub>-HAp were successfully obtained by foam replica method. With the increase of sintering temperatures, an increase in  $\beta$ -TCP was observed. Higher sintering temperatures are required for systems containing YSZ in order to achieve sufficient densification and satisfactory mechanical properties. The best mechanical properties were acquired in the case of the composite scaffolds based on doped hydroxyapatite and yttria-stabilized zirconia scaffolds after sintering at 1500 °C and gelatine coating, which is in line with the beginning hypothesis. The compressive strength of these scaffolds was 1019 kPa. Both kinds of scaffolds showed signs of bioactivity after the incubation in SBF for 7 days, with the Mg<sub>4</sub>Sr<sub>1</sub>-HAp samples being completely covered with newly formed HAp layer. The results of this study show potential application of the obtained scaffolds in bone regenerative therapy.

#### Acknowledgements

This work was supported by the Ministry of Education, Science and Technological Development of the Republic of Serbia (Contract No.451-03-68/2022-14/200135 and 451-03-68/2022-14/200287).

#### 5. References

- [1] R. Dimitriou, E. Jones, D. McGonagle, P. V.Giannoudis, BMC medicine, 9(1) (2011) 1.
- [2] J. H. Shepherd, D. V. Shepherd, S. M. Best, Journal of Materials Science: Materials in Medicine, 23(10) (2012) 2335.
- [3] W. Wang, K. W. Yeung, Bioactive materials, 2(4) (2017) 224.
- [4] C. T. Laurencin, A. M. A. Ambrosio, M. D. Borden, J. A. Cooper Jr, Annual review of biomedical engineering, 1(1) (1999) 19.
- [5] R. Govindan, G. S. Kumar, E. K.Girija, RSC Advances, 5(74) (2015) 60188.
- [6] A. R. Amini, C. T. Laurencin, S. P.Nukavarapu, Critical Reviews<sup>TM</sup> in Biomedical Engineering, 40(5) (2012) 363.

- [7] M. Mirkovic, L. Kljajevic, S. Filipovic, V. Pavlovic, S. Nenadovic, *Science of Sintering*, 52(4) (2020) 405-413
- [8] A. Faeghina, T. Ebadzadeh, *Science of Sintering*, 52(4) (2020) 469-479
- [9] M. Frasnelli, V. M.Sglavo, *Acta biomaterialia*, 33 (2016) 283.
- [10] W. Xue, K.Dahlquist, A. Banerjee, A. Bandyopadhyay, S. Bose, *Journal of Materials Science: Materials in Medicine*, 19(7) (2008) 2669.
- [11] D. Veljovic, T. Matic, T.Stamenic, V. Kojic, S. Dimitrijevic-Brankovic, M. J. Lukic, D.Janackovic, *Ceramics International*, 45(17) (2019) 22029.
- [12] A. Ressler, A.Žužić, I.Ivanišević, N. Kamboj, H.Ivanković, *Open Ceramics*, 6 (2021) 100122.
- [13] C. M. Mardziah, I. Sopyan, S. Ramesh, *Artif. Organs*, 23(2) (2009) 105.
- [14] T. Matic, M. L.Zebić, V.Miletić, I.Cvijović-Alagić, R.Petrović, D.Janačković, D.Veljović, *Ceramics International*, 48(8) (2022) 11155
- [15] F. Scalera, B. Palazzo, A. Barca, F.Gervaso, *Journal of Biomedical Materials Research Part A*, 108(3) (2020) 633.
- [16] C. Galli, E.Landi, S.Belletti, M. T. Colangelo, S.Guizzardi, *Applied Sciences*, 11(20) (2021) 9723.
- [17] E. M. Rivera-Muñoz, *Biomedical Engineering-Frontiers and Challenges*, (2011)75
- [18] V. Karageorgiou, D. Kaplan, *Biomaterials*, 26(27) (2005) 5474.
- [19] G. A. S. Kazi, R.Yamagiwa, (2020). *Restorative Dentistry & Endodontics*, 45(4) (2020) e52.
- [20] S. M. Kim, S. A. Yi, S. H. Choi, K. M. Kim, Y. K. Lee, *Nanoscale research letters*, 7(1) (2012) 1.
- [21] D. Janackovic, I. Petrovic-Prelevic, L. Kostic-Gvozdenovic, R. Petrovic, V. Jokanovic, D. Uskokovic, *Key Eng. Mater.* 192–195 (2001) 203.
- [22] I. Zalite, J.Grabis, E.Palcevskis, M. Herrmann, *IOP Conference Series: Materials Science and Engineering*, 18 (6) (2001) 62024
- [23] I. Sopyan, M. Mel, S. Ramesh, K. A. Khalid, *Science and Technology of Advanced Materials*, 8(1-2) (2007) 116.
- [24] A. L. Metze, A. Grimm, P. Noeaid, J. A. Roether, J. Hum, P. J. Newby, A. R. Boccaccini, *Key Engineering Materials*, 541 (2013) 31.

- [25] T. Reiter, T. Panick, K. Schuhladden, J. A. Roether, J. Hum, A. R. Boccaccini, *Bioactive materials*, 4 (2019) 1.
- [26] Q. Nawaz, M. A. U. Rehman, J. A. Roether, L. Yufei, A. Gruenewald, R. Detsch, A. R. Boccaccini, *Ceramics International*, 45(12)(2019) 14608.
- [27] T. Furusawa, T. Minatoya, T. Okudera, Y. Sakai, T. Sato, Y. Matsushima, H. Unuma, *International Journal of Implant Dentistry*, 2(1) (2016) 1.
- [28] G. Ayoub, D. Veljovic, M. L. Zebic, V. Miletic, E. Palcevskis, R. Petrovic, D. Janackovic, *Ceramics International*, 44(15) (2018) 18200.
- [29] B. Liu, P. Lin, Y. Shen, Y. Dong, *Journal of Materials Science: Materials in Medicine*, 19(3) (2008) 1203.
- [30] M. Dreßler, F. Dombrowski, U. Simon, J. Börnstein, V. D. Hodoroba, M. Feigl, M. Neumann, *Journal of the European Ceramic Society*, 31(4) (2011) 523.
- [31] A. Philippart, A. R. Boccaccini, C. Fleck, D. W. Schubert, J. A. Roether, *Expert review of medical devices*, 12(1) (2015) 93.
- [32] L. Liang, P. Rulis, W. Y. Ching, *Acta biomaterialia*, 6(9) (2010) 3763.
- [33] M. Bohner, B. L. G. Santoni, N. Döbelin, *Acta biomaterialia*, 113 (2020) 23.
- [34] D. J. Curran, T. J. Fleming, M. R. Towler, S. Hampshire, *Journal of Materials Science: Materials in Medicine*, 21(4) (2010) 1109.
- [35] T. Kokubo, H. Takadama, *Biomaterials*, 27(15) (2006) 2907.

## Сажетак

Ограниченост капацитета банака костију и ризик од инфекције су основни недостатци аутологних и алогених графтова, што отвара могућност новим синтетичким материјалима за примену у својству коштаних имплантата. Циљ овог рада је био процесирање, испитивање механичких својстава и биоактивности магнезијумом и стронцијумом допираних хидроксиапатитних (НАр) макропорозних носача, као и испитивање утицаја додавања цирконијум(IV)-оксида и превлачења желатином. Допирани наночестични хидроксиапатитни прах нанометарских димензија синтетисан је хидротермалном методом, а носачи су добијени методом реплике полимерног сунђера и синтеровани на различитим температурама. Итријумом стабилисан цирконијум(IV)-оксид (YSZ), синтетисан плазма технологијом, је коришћен као ојачавач калцијум-фосфатних макропорозних носача. Дефинисани су елементни састав, фазни састав, морфологија прахова и микроструктура носача, као и притисна чврстоћа носача са и без полимерне превлаке и биоактивност у симулираној телесној течности (SBF). Добијена је макропорозна структура са међусобно повезаним порима, а биоактивност у SBF је потврђена у свим случајевима. Најбоља механичка својства показали су композитни НАр/YSZ носачи превучени желатином, издржавши просечно оптерећење од 1019 kPa. Ови резултати подржавају идеју о примени добијених носача приликом регенерације костију и инжењерству коштаног ткива.

**Кључне речи:** хидроксиапатит, макропорозни носач, цирконијум(IV)-оксид, композит, инжењерство ткива.

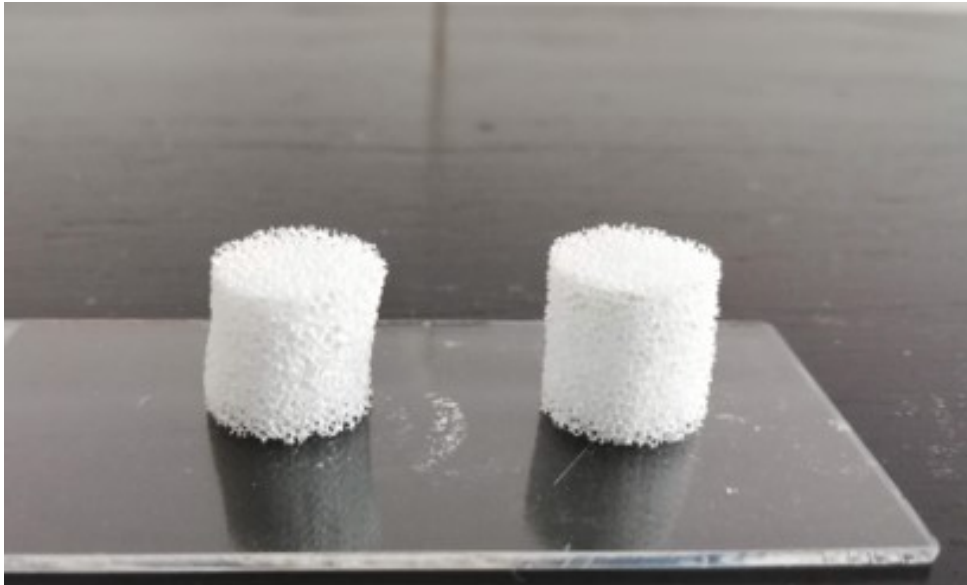


**Fig.1.** Polymer foams after dipping in paste

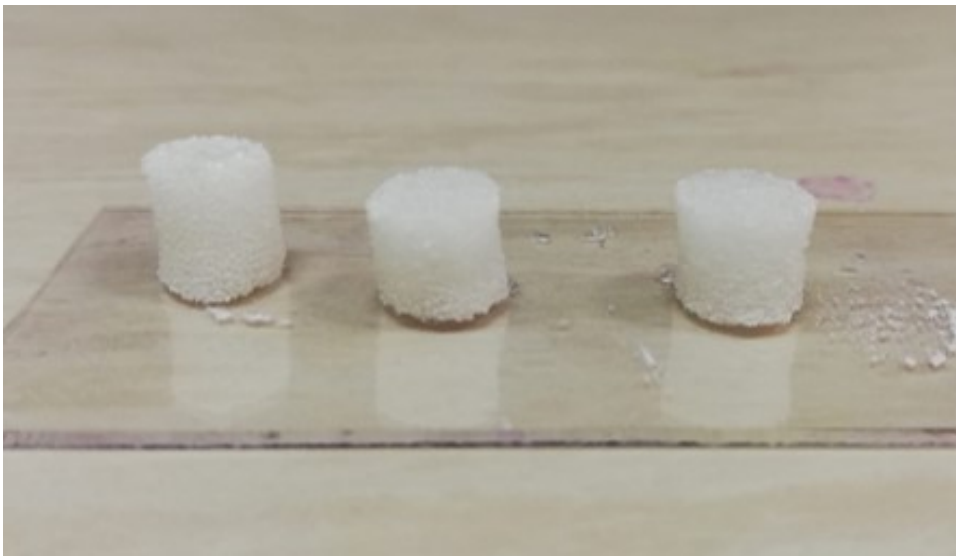


**Fig. 2.** Scaffolds after sintering

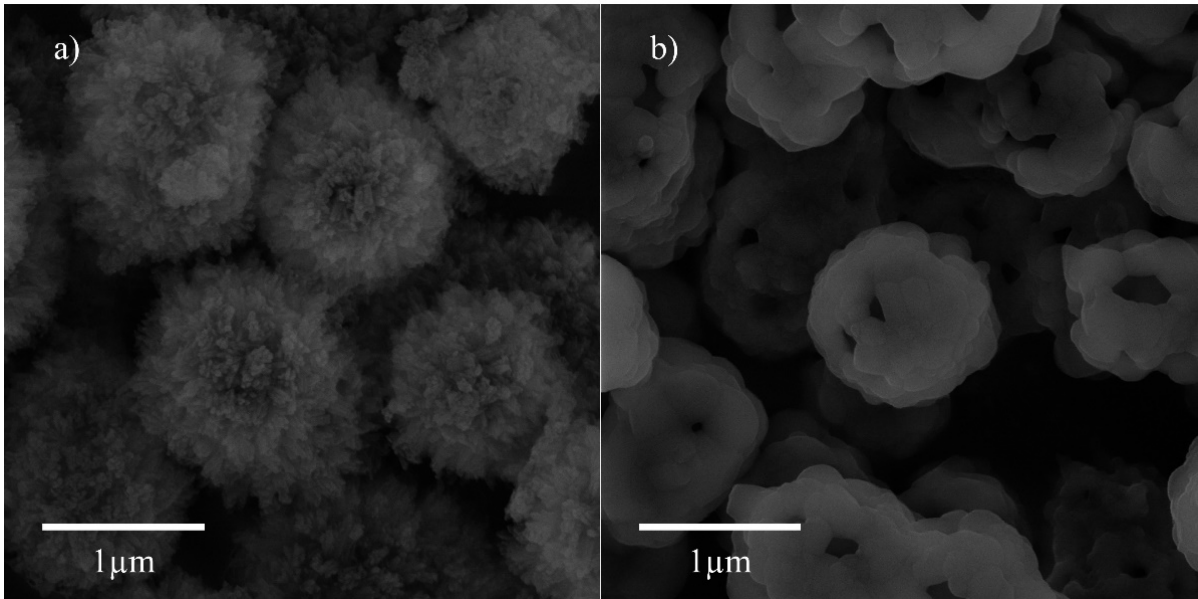


**Fig.3.** a) synthesized Mg<sub>4</sub>Sr<sub>1</sub>-Hap powder and b) calcined at 1000°C

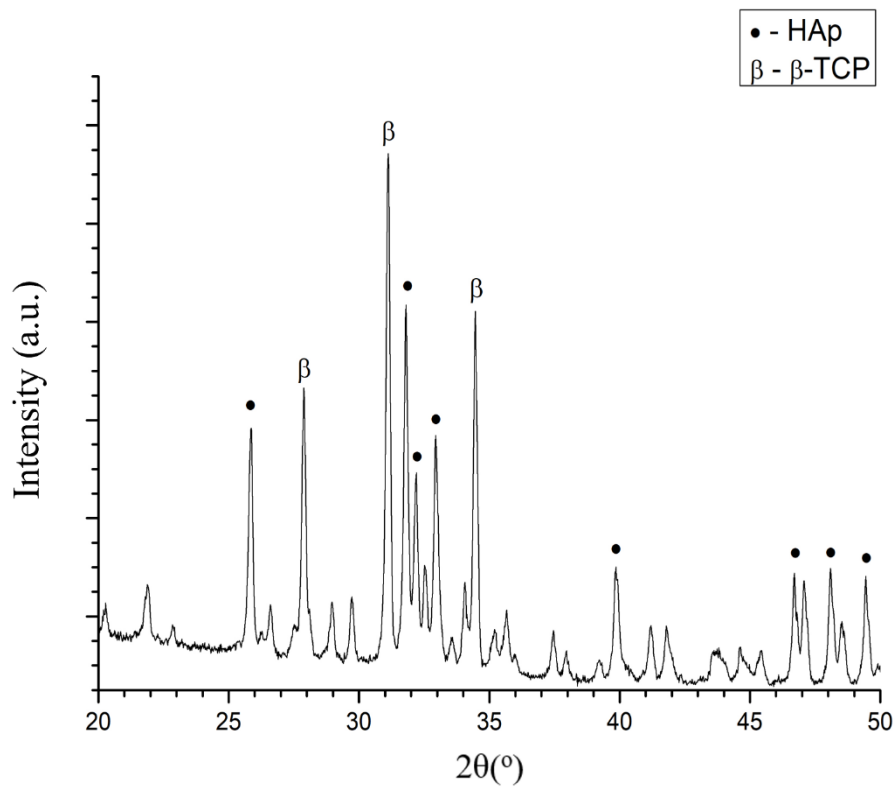


**Fig.4.** Diffractogram of the calcined Mg<sub>4</sub>Sr<sub>1</sub>-Hap powder.

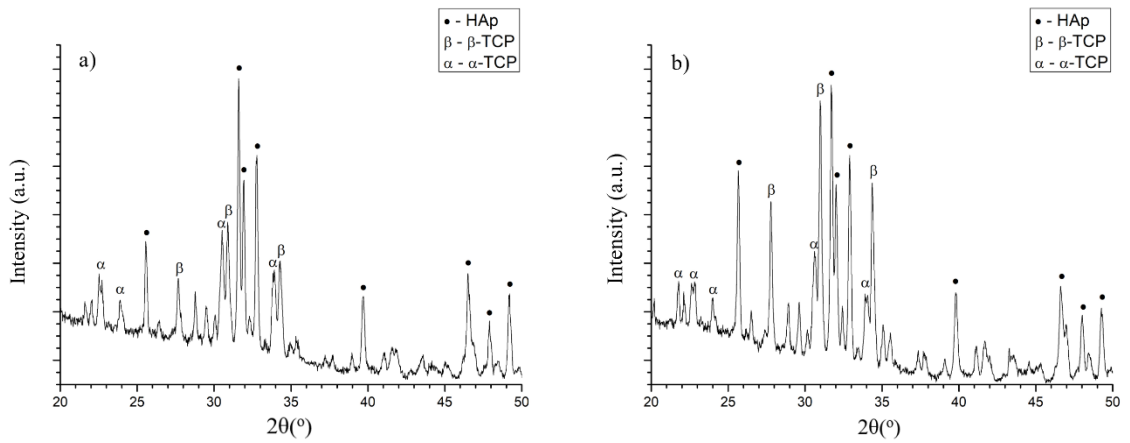


**Fig.5.** Diffractogram of the a) Mg4Sr1-Hap scaffold sintered at 1400°C and b) Mg4Sr1-Hap scaffold sintered at 1430°C.

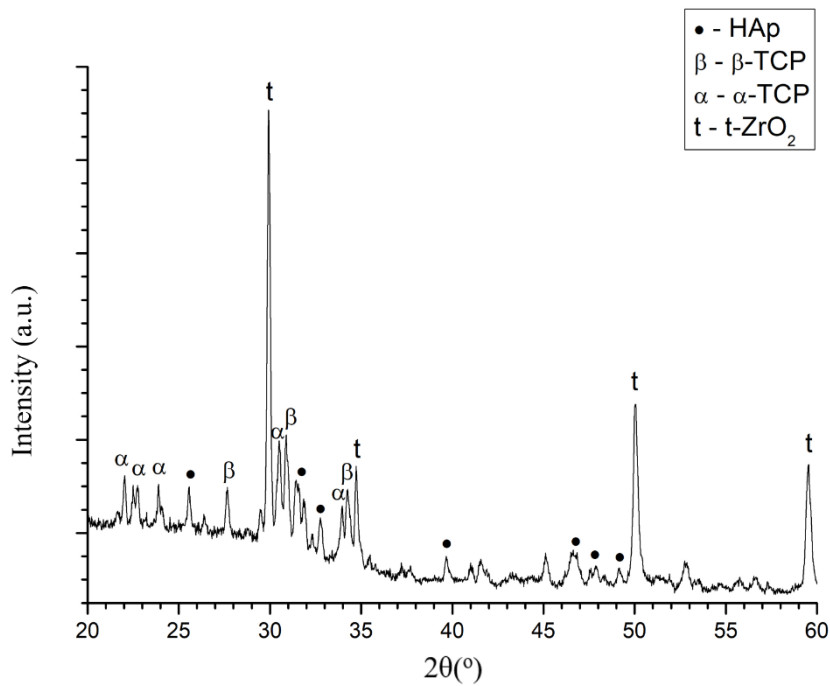


**Fig. 6.** Diffractogram of the Mg4Sr1-HAp/YSZ scaffold sintered at 1470°C.



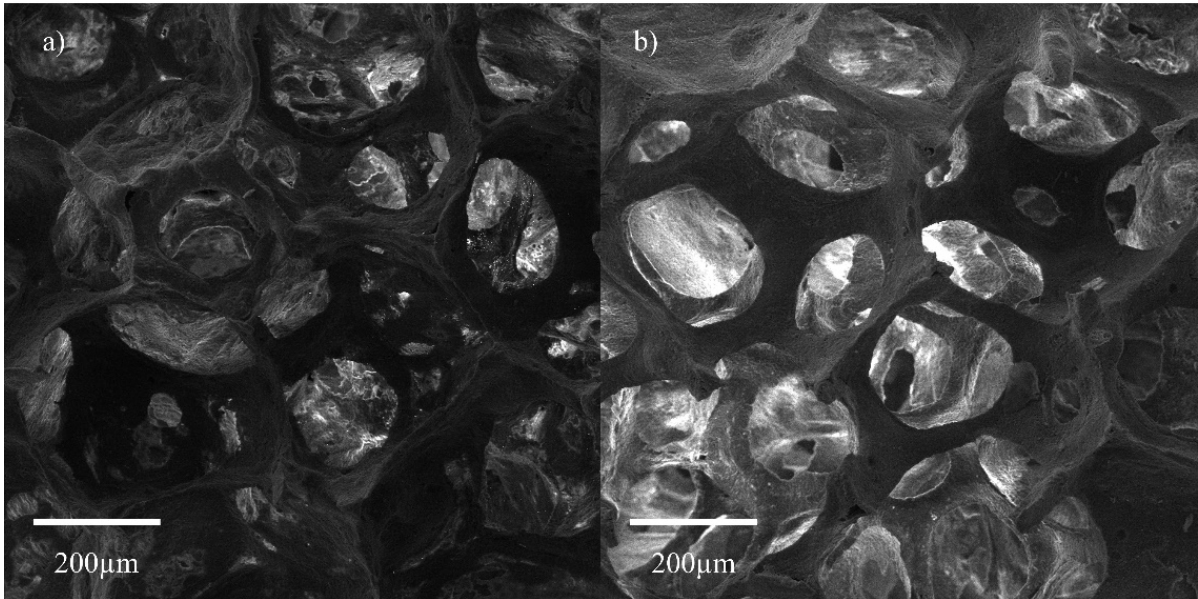


**Fig.7.**Microstructure of the a) doped Mg<sub>4</sub>Sr<sub>1</sub>-HAp and b) composite scaffolds

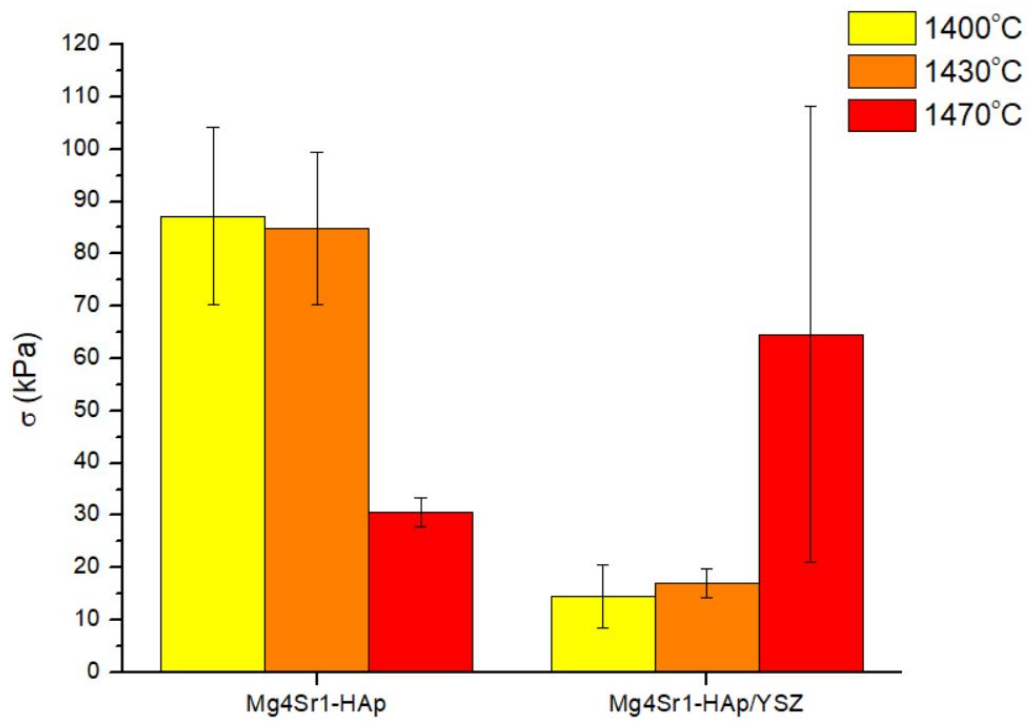


**Fig.8.**Compressive strength of the uncoated scaffolds

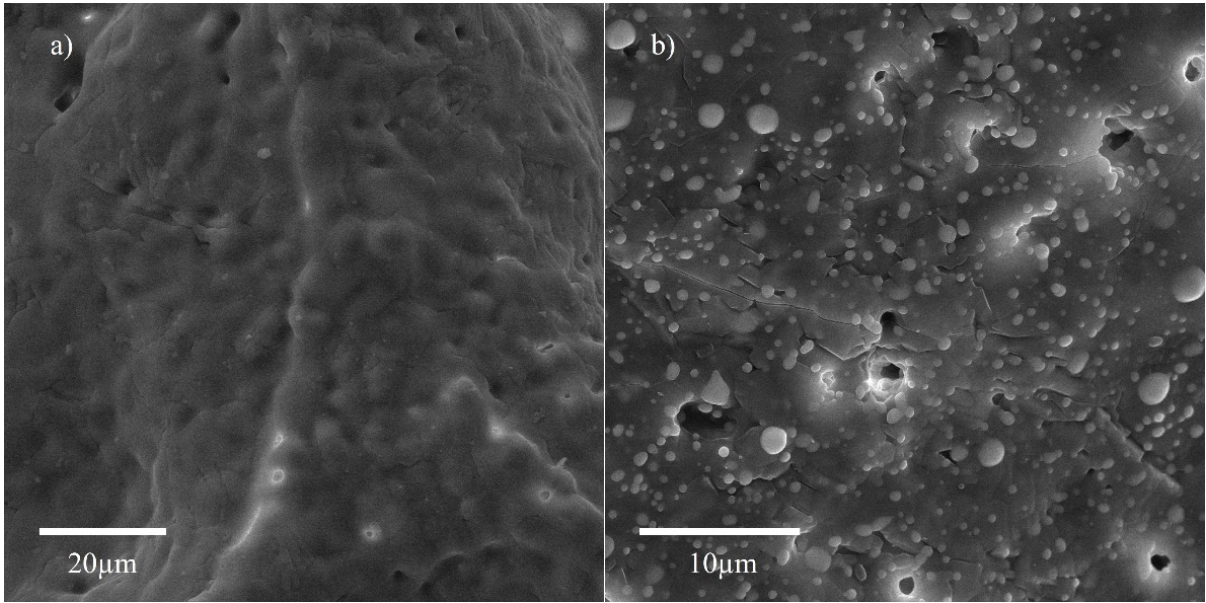


**Fig. 9.** Microstructure of the (a) doped Mg<sub>4</sub>Sr<sub>1</sub>-HAp scaffolds sintered at 1400°C and (b) composite scaffolds sintered at 1470°C

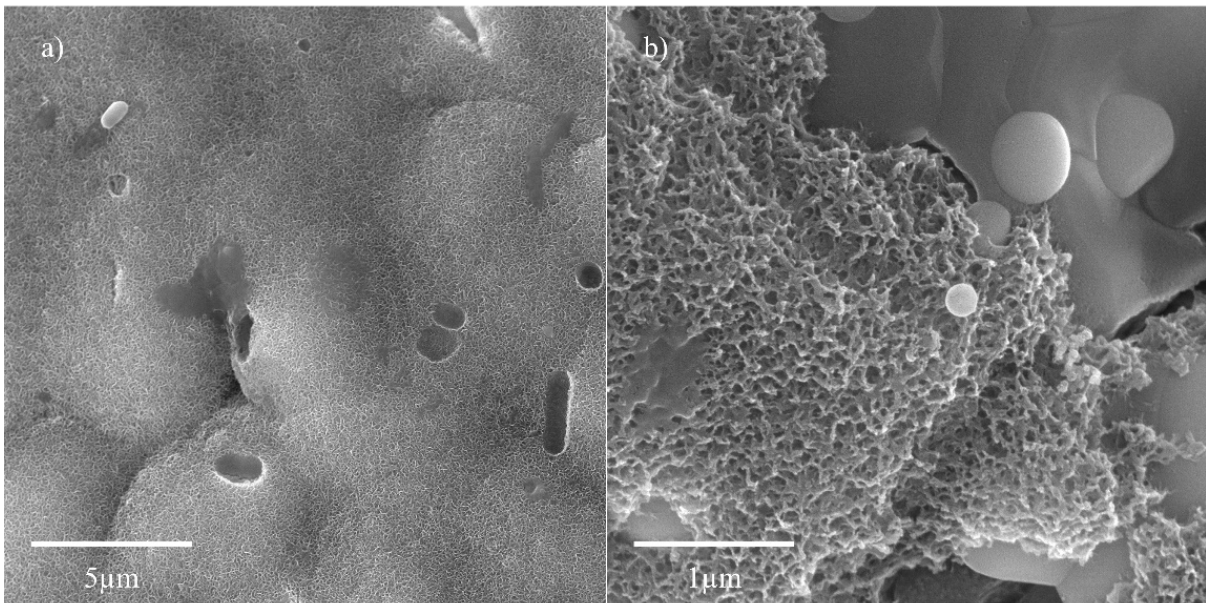


**Fig.10.** (a) Mg<sub>4</sub>Sr<sub>1</sub>-HAp sintered at 1400°C and (b) Mg<sub>4</sub>Sr<sub>1</sub>-HAp/YSZ sintered at 1470°C after 7 days in SBF.

**Tab. I** Reactants and their amounts

| <b>Ca(NO<sub>3</sub>)<sub>2</sub>·4H<sub>2</sub>O</b> | <b>Na<sub>2</sub>H<sub>2</sub>EDTA·2H<sub>2</sub>O</b> | <b>NaH<sub>2</sub>PO<sub>4</sub>·2H<sub>2</sub>O</b> | <b>urea</b> | <b>Mg(NO<sub>3</sub>)<sub>2</sub>·6H<sub>2</sub>O</b> | <b>Sr(NO<sub>3</sub>)<sub>2</sub></b> |
|---|--|--|-------------|---|---------------------------------------|
| 11,21 g   | 11,18 g  | 5,13 g   | 12,00 g     | 0,488 g   | 0,106 g                               |

**Tab. II** The phase composition of the Mg4Sr1-HAp samples after thermal treatments

| <b>Sample</b>                                  | <b>Phase composition</b> |            |            |
|--|--------------------------|------------|------------|
| <b>Mg4Sr1-HAp powder calcined at 1000 °C</b>   | 37 % HAp                 | 63 % β-TCP |            |
| <b>Mg4Sr1-HAp scaffold sintered at 1400 °C</b> | 52 % HAp                 | 30 % β-TCP | 18 % α-TCP |
| <b>Mg4Sr1-HAp scaffold sintered at 1430 °C</b> | 40 % HAp                 | 42 % β-TCP | 18 % α-TCP |